

International Conference on Space Optics—ICSO 2022

Dubrovnik, Croatia

3–7 October 2022

Edited by Kyriaki Minoglou, Nikos Karafolas, and Bruno Cugny,



Low reflectivity, reference pixels in Mercury Cadmium Telluride infrared arrays



Low reflectivity, reference pixels in Mercury Cadmium Telluride Infrared Arrays

Dan Owton, Les Hipwood, Jim Gordon, Audrey Cooper, Emma D'Arcy, Marcus Lee & Matthew Hicks

Leonardo UK Ltd, Southampton, Hampshire, UK, SO15 0LG

Abstract

Low reflectance, blinded HgCdTe pixels would allow the effects of drifts in the supply voltage and operating temperature to be accounted for when trying to resolve very faint objects. This paper describes the progress of an ESA / Leonardo contract in developing such a layer. The structure chosen offers significant levels of blocking for the masked pixels as well as minimal reflection to prevent optical cross-talk to neighbouring pixels.

Keywords: *Leonardo, MCT, Avalanche Photo – diodes, APD, Fabry Perot*

1.0 Introduction

Any detector aimed at very high sensitivity detection of faint sources, such as the search for exoplanets will benefit from reference pixels used to compensate for the effect of temporal noise sources within the signal chain. Other available reference pixel architectures use dummy pixels that are not connected to infrared sensitive photodiodes - this only provides compensation for voltage drifts and because of imperfect capacitance matching is not ideal. Generating reference pixels by blocking the incoming infrared radiation results in perfect matching so that both operating voltages and changes in FPA temperature can be fully compensated. A low reflectivity opaque layer applied to a small percentage of the pixels towards the perimeter of the focal plane array, would provide a dark current reference in the infrared photon detector array. Conventional infrared blacks are thick, rough, textured coatings and would not be compatible with Leonardo hybrid arrays. Alternative, visible blacks, for example anodised aluminium, become reflective in the infrared. To be compatible, the opaque mask would have to be thin film.

This paper describes the progress of an ESA / Leonardo contract (reference 4000133646/20NL/AR) in developing such a layer optimised for use with cooled detectors, rather than room temperature structures referred to in previous literature. In [RD1] and [RD2] an MIM (metal, insulator, metal) structure was investigated. This consisted of an opaque metal reflector, quarter wave dielectric and thin metal absorber, impedance matched to free space. This is the system to be investigated in our work, making use of chrome, zinc sulphide (ZnS), and Nichrome (NiCr) films respectively; these materials being readily available at Leonardo, Southampton. The principle of our preferred coating system is firstly to minimise transmission of light to the active pixels by means of the opaque chrome coating. Then, in order to minimise opaque layer reflection within the operating band, the same quarter wave ZnS antireflection coating as used in the active detector area of the focal plane array (FPA) is deposited over the opaque metal layer followed by a 377ohm/sq NiCr layer over the ZnS. This NiCr layer would be impedance matched to free space so that it absorbs 50% and transmits 50% of the incident light with (in the ideal case) zero reflection. Destructive interference between the light reflected from the opaque layer and the incident light at the NiCr coated surface gives a very low reflectivity from this structure at the band centre.

2.0 Planned Structure

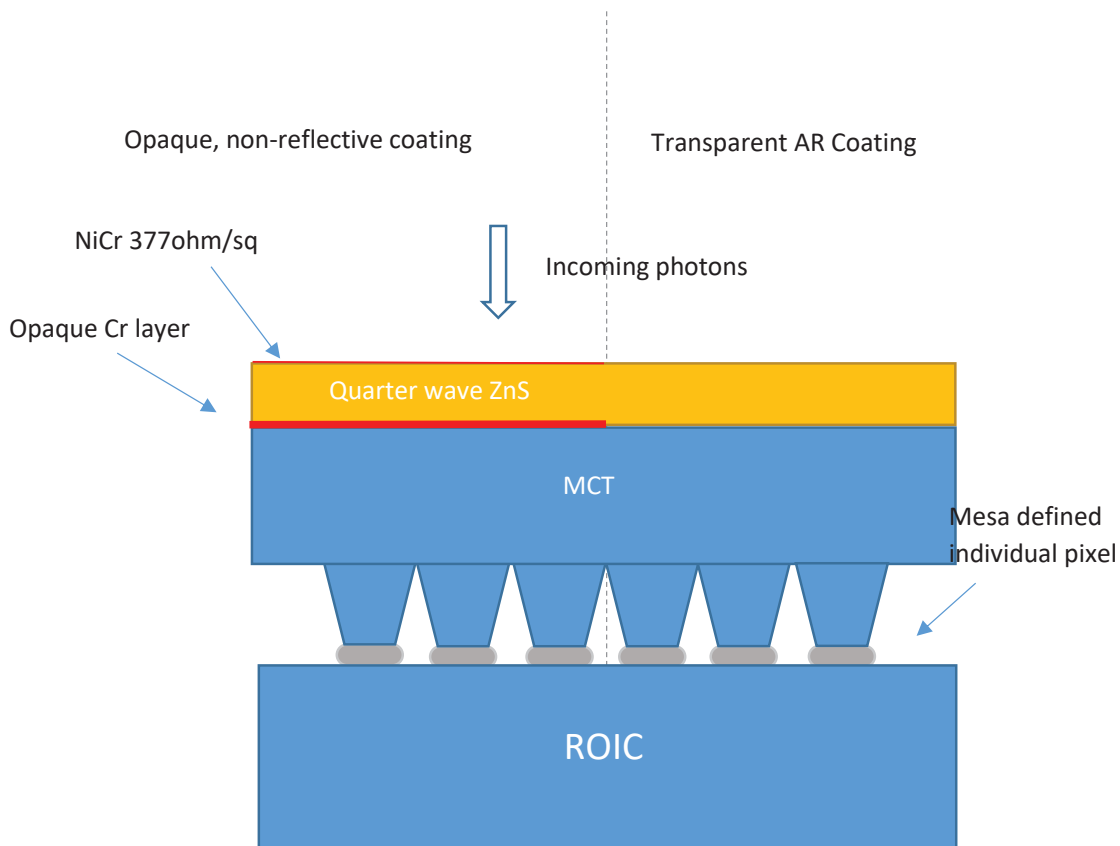


Figure 1: planned layer design. The chrome absorber is expected to be around 100nm for long wave device and around 150nm thick for short wave devices to achieve a masking effect of $1E-4$

A thin film absorber, based on a Fabry Perot structure has been fabricated directly above pixels located around the edge of the focal plane. This is based on an MIM structure, with the outer metallic layer impedance matched to free space to minimise the reflectivity of the new surface.

Initial trials focused on optimising the performance of the three layers, whilst subsequent work has manufactured arrays including the new structure in both short wave (centred around $1.5\mu\text{m}$) and long wave ($8-10\mu\text{m}$) arrays. These arrays were then subjected to environmental stresses typical of that required for a space flight programme.

3.0 Initial Trial Layers

Trial samples have been manufactured on both short wave and long wave arrays. In both cases, the focus has been on similar parameters: minimising the transmission of the light in the waveband in question, creating an outer metallic layer of a suitable resistivity and producing a robust layer, capable of being manufactured using existing equipment and processes.

3.1 Transmission

Arrays have been manufactured with the chrome masking layer over the complete structure. By varying the layer thickness and measuring the performance of the array across a range of flux levels, the effect of dark current and stray radiation are accounted for and the transmission of the thickness in question can be deduced. Our process uses chrome for this layer, due to it being a readily available process within the array fabrication clean room at Leonardo, Southampton.

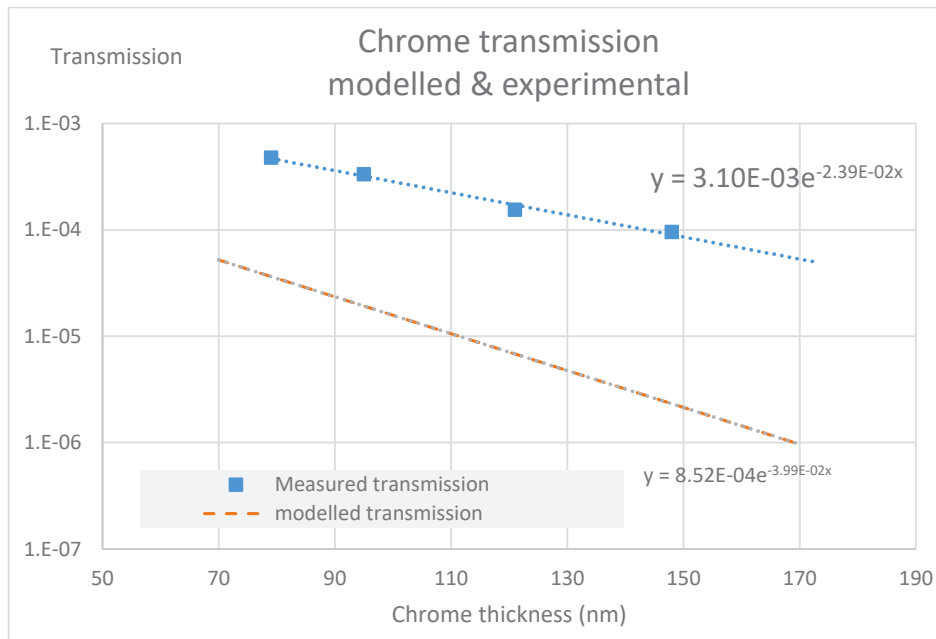


Figure 2: Modelled and experimental transmission. The differences between the two curves are likely due to differences in the Cr structure in deposited films (grain size, voids, purity etc). Experimentally, 150nm of Cr can be seen to offer masking effect of a factor of around 1×10^{-4} in the transmission of long wave (10 microns) radiation.

3.2 Reflectivity

To complete the Fabry Perot structure, a thin layer is deposited with a resistivity of the layer matched to that of free space, i.e. $377\Omega/\text{sq}$. The expected performance of the layer can be modelled using an equation published by Parsons/Pedder paper [RD2]:-

$$a = \frac{4f}{[(f + 1)^2 + n^2 \cot^2(2\pi nd/\lambda)]}$$

where a is the absorption of the structure, f is $377/R_f$, R_f is absorber layer sheet resistivity in Ω/sq , n is the dielectric refractive index, d is the thickness of the dielectric & λ is the wavelength of the radiation.

The transmission for an ideal layer is presented in figure 3.

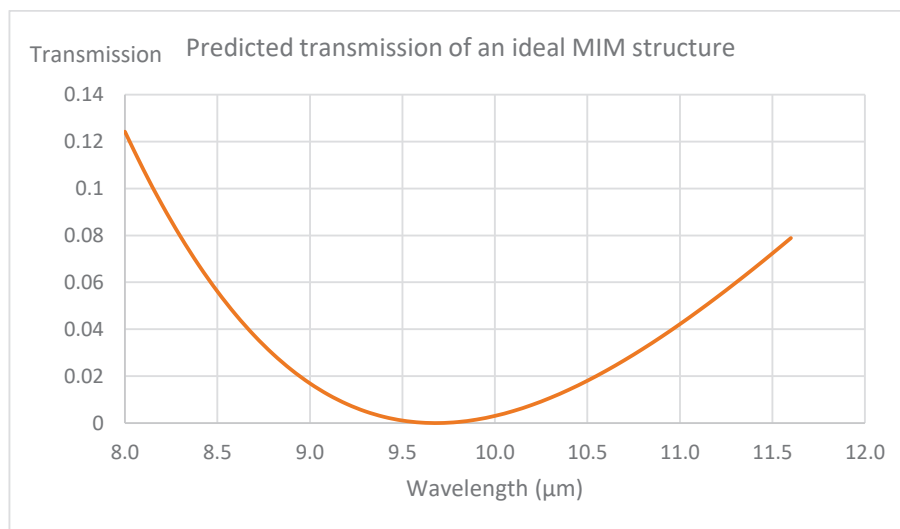


Figure 3: Modelled transmission curve of the planned MIM structure, optimised for long wave radiation ($377\Omega/\text{sq}$, Anti-reflection coating of $1\mu\text{m}$ ZnS).

3.3 Transmission

Prior to developing the deposition process parameters for the NiCr process, a literature review suggested a thickness of around 50nm would achieve the desired resistivity. In general, these papers suggested that a lower deposition pressure, higher power and higher gas flow process should lead to higher resistance. A number of trial runs were carried out to optimise the process parameters to achieve the desired resistivity. Initially samples were measured using a standard room temperature four-point probe. Additionally three of the final samples were cooled to 80K using a vacuum dewar to confirm the offset caused by the reduction in measurement temperature.

Thickness measurement 1 (nm)	Thickness measurement 2 (nm)	Average thickness (nm)	Measured resistivity room temperature, Ω/sq
121.6	118.8	120.2	8.7
33.1	35.2	34.2	21.0
27.0	28.5	27.8	49.8
12.5	13.0	12.8	158
11.2	11.5	11.4	141
10.7	10.9	10.8	208
9.4	-	9.4	302

Table 1: Resistance data for different thicknesses at room temperature. It can be seen from the data that the required thickness is significantly thinner than expected from the literature studies. At present, the reason for this is not understood and is subject to further work.

The three NiCr samples cooled using a liquid nitrogen dewar were all coated using the same process as that used to achieve the 302 Ω/sq resistivity sample. These samples consisted of a rectangular glass microscope slide, with gold pads at either end, creating a square uncoated area. The NiCr was applied across the whole slide, with wirebonds applied directly to the gold/NiCr surface. Standard samples, i.e. those used for the room temperature measurements were also coated and measured in the same deposition runs.

3.3.1 Cooled results

Sample No	1	2	3
Resistivity (4 point probe) Ω/sq	282	269	268
Coolable Sample (Warm) Ω	252.5	239.3	241.0
Coolable Sample (Cold) Ω	246.8	234.0	236.0

Table 2: The average cooled sample resistivity is around 239 Ω . Cooling the sample to its likely operating temperature of 80K, reduced the resistance by around 2% as might be expected.

Samples manufactured using all 3 layers (i.e. 150nm Cr, 1.0 μm ZnS and 10nm of NiCr) have been used to measure the reflectivity of the proposed layer.

Two of these samples were subjected to a measurement of reflectivity using an Agilent FTS 40 spectrometer. This FTIR spectrometer allows the degree of reflection to be measured over a range of angles. In addition, the use of a UMA 600 spectrometer allows the sample to be cooled to the expected operating temperature (80K) and the reflectivity measured, although this equipment only allows measurement normal to the beam.

3.4 Reflectivity results

Cooled

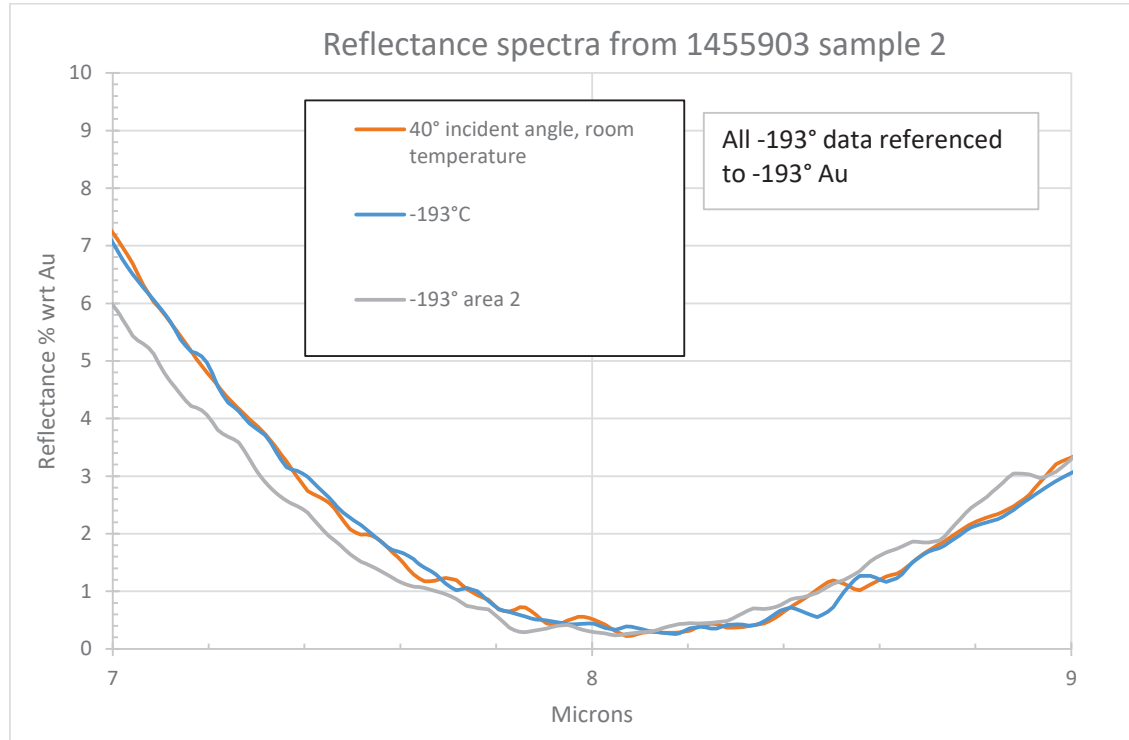


Figure 4: Cooled sample reflectivity data, using a structure optimised for LW Mercury Cadmium Telluride (MCT), note the good agreement between the two cooled data sets (blue and grey lines). Area 2 refers to a second measurement point made on the sample. The orange line refers to a measurement made at room temperature with the sample angled at 40 degrees to the beam.

Figure 4 demonstrates the potential of the structure to achieve required performance, despite the NiCr layer not being as high resistance as would be desired for optimum performance.

4.0 Arrays manufactured to the complete design

Samples were then manufactured using production standard MCT and ROICs. These samples were fabricated using standard production equipment and processes, up to the point of applying the mask for the opaque layer. A number of arrays were made using a recipe of:-

Chrome: 150nm, planned to reduce the transmission of long wave light by 99.99%

Zinc Sulphide: 1 μ m, used as an antireflection coating for the bulk of the array and as the insulator in the MIM structure.

Ni-chrome: 10nm, designed to absorb 50% of the incoming radiation and transmit 50%, theoretically reducing the reflected light to zero.

The mask for this layer was designed to create a variable thickness mask of 10, 20, 30 and 40 pixels around the four sides of the central area. Once completed, each sample was subjected to the standard electro-optical tests and the effect of the masking assessed.



Figure 5: A plot of the output of a masked long wave device (640 x 512 24 μ m) which consists of a greyscale (lighter for higher signal and darker for lower signal). Masked pixels can be seen as a dark border, 10 columns to the left, 30 to the right, 20 rows at the top and 40 at the bottom. The array in question is imaging a flat field at 40°C.

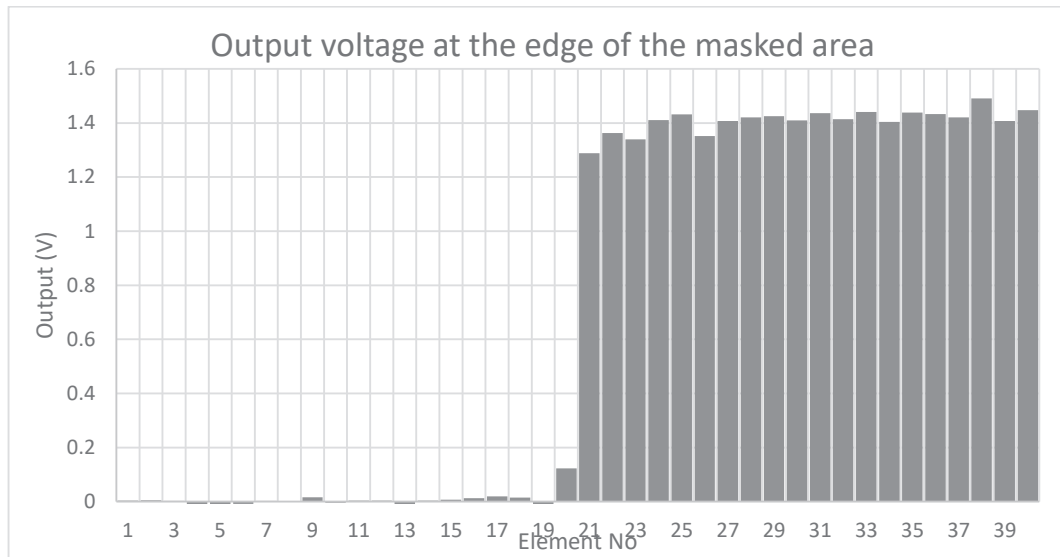


Figure 6: An expanded image of the top of the image of a single column of uncorrected pixels (Column 90). It can be seen that the column might have a degree of optical crosstalk, perhaps limited to approximately 10%. However, this is limited to only 1 or 2 rows, further work is planned to assess this.

5.0 Conclusion

Leonardo have developed a method to mask a few pixels, typically towards the edge of the pixel array plane, which has the potential to increase the sensitivity of a focal plane array. The technique has the advantages that is it compatible with current array processes, and offers a simple route to space qualification. Further work is required to increase the resistivity of the NiCr layer and hence to reduce the amount of stray light reflected from the surface to further improve the performance of the sensor. However, the new structure has demonstrated the potential to significantly improve the ability of the sensor to detect faint signals by allowing the effects of drifts in supply voltage, sensor temperature and changes in straylight to be subtracted from the raw data.

References

- [RD1] “Thinfilm infrared absorber structures for advanced thermal detectors”. A.D. Parsons and D.J. Pedder. *Journal of Vacuum Science and Technology A* 6, 1686 (1988)
- [RD2] “Application of Interferometric Enhancement to Self-Absorbing Thin Film IR Detectors”. K.C. Liddard. *Infrared Phys. Vol 34, No 4, pp 379-387 (1993)*

Acknowledgement

Thanks to Dr Kyriaki Minoglou and ESA for their support under ESA Contract 4000133646/20NL/AR

Thank you to all at Leonardo who assisted with the design, manufacture and testing of the devices used in this project.